Vortices and critical current in disordered arrays of Josephson junctions

P. L. Leath and W. Xia
Department of Physics and Astronomy, Rutgers, The State University of New Jersey, Piscataway, New Jersey 08855-0849
(Received 2 May 1991)

The breakdown phenomena of disordered arrays of two-dimensional resistively shunted Josephson junctions driven by dc external current are studied numerically at zero temperature and zero magnetic field. First we report on perfect arrays with large linear defects (rows of missing junctions). We show the formation of vortices on the defect tips, the depinning of these vortices at the critical current, the production of Josephson oscillations by the motion of these vortices and additional transitions as breakdown occurs row by row in adjacent rows. Next we study the funnel defect to show that, in this model, local confined (nonspanning) regions of the sample cannot become normal until an entire spanning or global region or vortex path across the sample can be found. In randomly disordered samples, global breakdown means that the most critical defect region of the sample cannot become normal until a connected global path of such regions across the sample can become normal and develop a voltage. This point of global breakdown defines the critical current i_c in randomly disordered arrays. At currents just below i_c, large regions of the sample may be critical or near critical, with vortices ready to depin from their defects in a form of self-organized criticality. It may be possible to stimulate this near depinning by external probes in this situation. We also study the statistics of an ensemble of 800 arrays of 25×25 junctions at $p=0.90$ to observe the failure distribution $F(i)$ (or critical current distribution) within the ensemble. We find consistency with the modified Gumbel form for $F(i)$, as in the case of linear problems, despite the nonlinearity. Finally we observe the average voltage $\langle V\rangle$ versus applied current i for the samples in the ensemble and find that $\langle V\rangle$ varies as $(i-i_{\langle V\rangle})^x$, where $x=3.10\pm0.10$.

I. INTRODUCTION

Breakdown processes in various randomly disordered systems have been the subject of extensive study over the past few years[1–3] and are now becoming quite well understood. The electrical, dielectric, and mechanical breakdown strength and the overall failure probability distribution function of these systems have been calculated by numerical simulations and are consistent with the predicted scaling laws using the statistics of extremes.[4] In this theory the breakdown is caused by the most critical defect, or region of defects, and understanding the statistics of these most critical defects or regions is vital to understanding the statistics of breakdown. Similar results apply to the critical current in linearized models of superconductivity.[5] In all these models there is a linear relation between the load and response, up to a critical breaking point; thus we shall call them linear models.

For many examples in nature, nonlinearity is important and affects the breakdown process. This is the case for superconductivity where the nonlinearity dramatically effects the breakdown phenomena at the critical current. In order to understand the effects of this nonlinearity, we have chosen to study the case of superconductivity in disordered arrays of Josephson junctions at zero temperature and zero external magnetic field. Granular superconductors consists of superconducting grains connected by intergrain proximity-effect tunneling through weak links. These weak links can be modeled by arrays of tunnel junctions.[6] For overdamped systems, such as superconducting thin film, these links can be modeled by resistively shunted Josephson- (RSJ-) junction arrays.[7] Recently, it has been found that high-T_c ceramic superconductors, especially in their polycrystalline form, behave in many ways like random arrays of weak links.[8]

In this paper we continue the study reported earlier.[9,10] We shall consider here only the case of two-dimensional arrays of superconducting grains which are located on the sites (nodes) of a square lattice. Each node is connected to its nearest neighbors by bonds occupied by RSJ junctions. The RSJ junctions (bonds) are assumed to be identical, and disorder is introduced by randomly removing junctions (bonds). The numerical techniques used here are similar to those of several previous authors.[9–11] Since it has recently become relatively routine to study the properties of such Josephson junction arrays experimentally,[12] many of the results and phenomena reported here should be observable in real systems.

In Sec. II we introduce the model and describe the numerical method used to solve the dynamical equations of motion for the inhomogeneous arrays. In Sec. III we describe our results for a perfect array with a single defect of varying size and shape. Understanding these simple systems is critical to understanding the randomly disordered systems. Part of the section is an elaboration of the brief description given previously.[9] In Sec. IV we present and discuss our results for randomly disordered systems of various models. Section V contains our conclusions.

II. MODEL

The superconducting grains are assumed to occupy uniformly the sites (nodes) of a square lattice. Each grain

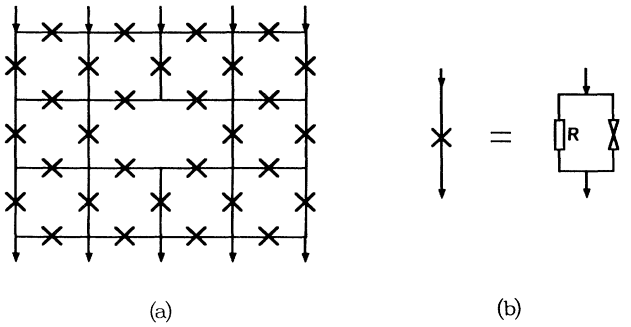

FIG. 1. (a) 5×4 junction array with a single defect (single missing junction). (b) Each resistively shunted junction can be considered as a microbridge and a resistor in parallel.

(site) is described by a complex superconducting order parameter $\Delta=\Delta_0 e^{i\varphi}$, where Δ_0 is constant for all grains and φ varies from grain to grain. We assume that each grain is coupled only to its nearest-neighboring grains by the resistively shunted Josephson junctions (bonds). Figure 1(a) shows a small 4×5 array with a single missing bond. The applied external current $I^{\rm ext}$ flows in at the top and out at the bottom of the array. Each junction, as illustrated in Fig. 1(b), can be considered as a resistor and a microbridge in parallel. For sufficiently small current it is obvious that all the current is in the form of supercurrent and there is no net voltage across the sample. As the current in any junction exceeds the maximum supercurrent I_0 that can flow (as defined below), some current must flow through the resistor and thus produces a net average voltage and dissipation. Here the charging effect, which would produce hysteresis in the junctions, has been neglected; this approximation is valid for proximity-effect junctions.[13] This approximation certainly makes the computations much easier and well defined because the hysteresis causes the computer to arbitrarily jump between the various metastable solutions. The current-conservation rule for a single junction is

$$I_0\sin(\varphi_1-\varphi_2)+\frac{h}{2eR}\left[\frac{d\varphi_1}{dt}-\frac{d\varphi_2}{dt}\right]=I_{12}\ , \tag{1}$$

where I_0 is the maximum supercurrent that can flow through the junction between grains 1 and 2, and φ_1 and φ_2 are the phases of the respective grains; R and I_{12} are the normal resistance and total current flowing between the two grains. On the left-hand side of Eq. (1), the first term is the Josephson supercurrent[14] and the second term is the normal current due to the voltage caused by the time-dependent phases between the grains. After defining a dimensionless time $\tau=2eRI_0t/h$ and current density $i^{\rm ext}=I^{\rm ext}/I_0$, the dimensionless phase equation of the kth grain of an array with identical junctions is given by

$$\sum_l\left[\frac{d\varphi_k}{d\tau}-\frac{d\varphi_l}{d\tau}\right]=i_k^{\rm ext}-\sum_l\sin(\varphi_k-\varphi_l)\ , \tag{2}$$

where the summation is over nearest-neighbor sites l and $i_k^{\rm ext}$ is the normalized externally applied current at site k. Equation (2) can be written in the generalized matrix form

$$G\frac{d\varphi}{d\tau}=C(\varphi)\ . \tag{3}$$

External currents are only supplied or withdrawn from the top and bottom rows, so that $i_k^{\rm ext}=0$ except for k's at the top and bottom of the array. The set of Eqs. (3) for each site are then solved by multiplying Eq. (3) by the matrix-integration factor G^{-1} and integrating numerically using a fourth-order Runge-Kutta integration scheme with appropriate initial phases $\varphi_i(0)$. This technique, which was used by Chung, Lee, and Stroud, is equivalent to that used by Shenoy and by Mon and Teitel for perfect arrays.[11] The disordered arrays, discussed later, are obtained by randomly removing a finite fraction of junctions and therefore creating random defects. As a check, we consider the case of a perfect square array of identical junctions with uniform initial condition for Eqs. (2). In this case the array behaves like a single giant junction;[15] i.e., for the external current density i less than $i_c=1.0$, there is no voltage across the sample; for i greater than i_c, the voltage across all junctions pulse in unison with the phase difference across any junction behaving like a staircase of steps versus time with a regular period[16] between steps:

$$T=\frac{h\pi}{eR}(i^2-i_c^2)^{-1/2}\ . \tag{4}$$

The time-averaged voltage over several periods is[16] $V=NR(i^2-i_c^2)^{1/2}$, where N is the number of junctions in the vertical direction. As the external current becomes very large, the steps become smaller and smaller and merge into a steady ramp so that the I-V curve shows ohmic behavior of an array of normal resistors.

III. PERFECT ARRAY WITH SINGLE DEFECTS

A. Linear defects

The situation is substantially different when there are defects present. To study this effect we first introduce a horizontal linear defect or slit by taking one [Fig. 1(a)] or several adjacent vertical junctions out of the central row of the uniform array. The current thus must flow around the defect, and therefore the current density near the defect tips is enhanced. When the external current is below the critical current of the sample, the phases of the grains are constant in time, although inhomogeneous in space (reflecting the current enhancement near the defect tips), and all the currents are in the form of supercurrents, and thus there is no voltage across the sample. When the current is small the supercurrent distribution is approximated by a dipole distribution about the defect as in the linearized problems.[2,5] Because of the current enhancement at the tip of the defect, the junction closest to the defect will first reach its maximum current $i_0=1.0$. We define i_v to be the applied current for which the super-

current in the most critical junction(s) (i.e., those carrying the most supercurrent, which in this case are at each end of the defect) reach $i_0=1.0$. As the external current is increased above i_v, we find that this nonlinear system (unlike the linear models) does not show any dissipation, but rather the current is redistributed outward, away from the defect by the formation of a vortex (or antivortex) attached to each end of the defect. The formation of vortices at each end of the defect is the result of the coherence and nonlinearity present in this model. This feature was absent in the linear model studied by Leath and Tang[5] and others.[1-3] The physical consequence of the vortex formation is that the vortex current tends to cancel the supercurrent in the junction closest to the defect and add to the current in the junctions farther out. This makes the current distribution near the defect more flat as current is shared with the farther neighbors. In Fig. 2 we show the supercurrent distribution versus position away from the defect tip along the axis of the defect, both below (where it approximates a $1/r^2$ dipole distribution) and above i_v, for a 35×16 junction array with defect length $A=10a$, where a is the lattice spacing.

Once the pinned vortices are formed at the tips of the defect, they will experience a Lorentz force $F_L \propto J\varphi_0/c$, perpendicular to the external current, where φ_0 is the vortex quantum, which is 2π in this case, and J is the external current density at the center of the vortices.[17] When the external current reaches i_c, the Lorentz force on the vortex equals the pinning force and the vortex breaks free and starts to move under the influence of the Lorentz force and thus, through $d\varphi/d\tau$, produces a voltage across the sample. Therefore, i_c is the critical current at which a voltage first appears. Of course, the vortex and antivortex move away from each other in directions perpendicular to the transport current. In Fig. 3 we plot the magnitudes of the horizontal component of the supercurrent versus lattice position at different times for junction arrays with periodic boundary conditions in the horizontal direction. The length of the defect is $10a$; the width is a (one lattice spacing). The graphs in Fig. 3 represent snapshots of a 35×34 array at different times (in units of τ) with external current $I=0.50>i_c=0.472$. One can see clearly the periodic creation and motion of the vortices (because of the horizontal periodic boundary condition, the vortex and antivortex actually annihilate each other at the boundaries). In the present problem the external current is kept steady, and therefore there are constant creation and depinning of the moving vortices with a period T, which determine the spacing between moving vortices. The rate of phase change, $d\varphi/d\tau$, monitored here at a site in the top row of the array, pulses periodically, corresponding to the periodic motion of the vortices in the central row (see Fig. 4). That is, when a defect is present the Josephson oscillations are created by the motion of the vortex lines. Since the voltage is, by definition, proportional to the time average of the phase change over a period, it is inversely proportional to the period T between pulses. We find that the period is given by $T=T_A(i^2-i_c^2)^{-1/2}$, similarly to Eq. (4), for i above and sufficiently close to i_c and where T_A depends on the

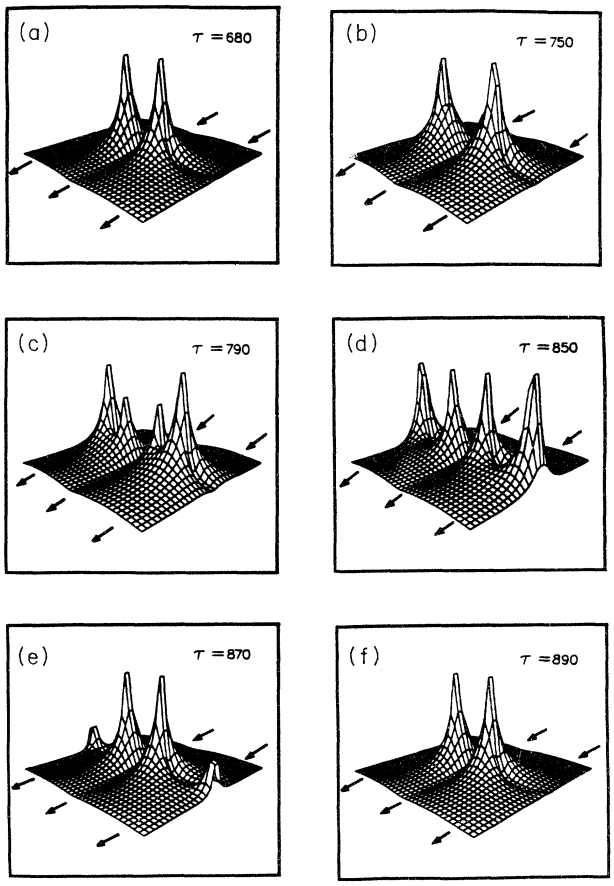

FIG. 3. (a)–(f) Snapshots of vortex movement in a 35×34 array with a single linear defect ($A=10a$) at $i>i_c$ at different times indicated by τ. Picture (f) is identical to (a), and the (a)–(f) process repeats indefinitely. The plot is of the supercurrent in the horizontal bonds vs position in the array.

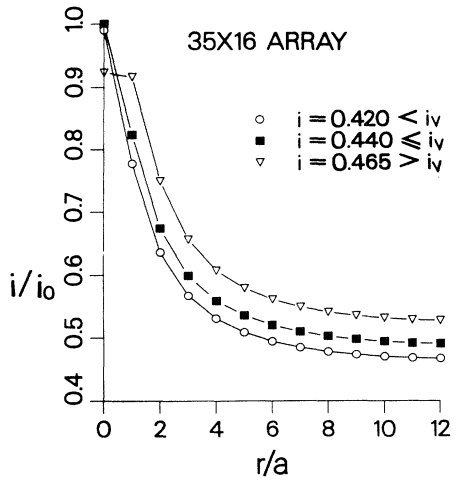

FIG. 2. Supercurrent i/i_0 in the vertical junctions in the central row vs distance r from the tip of the defect.

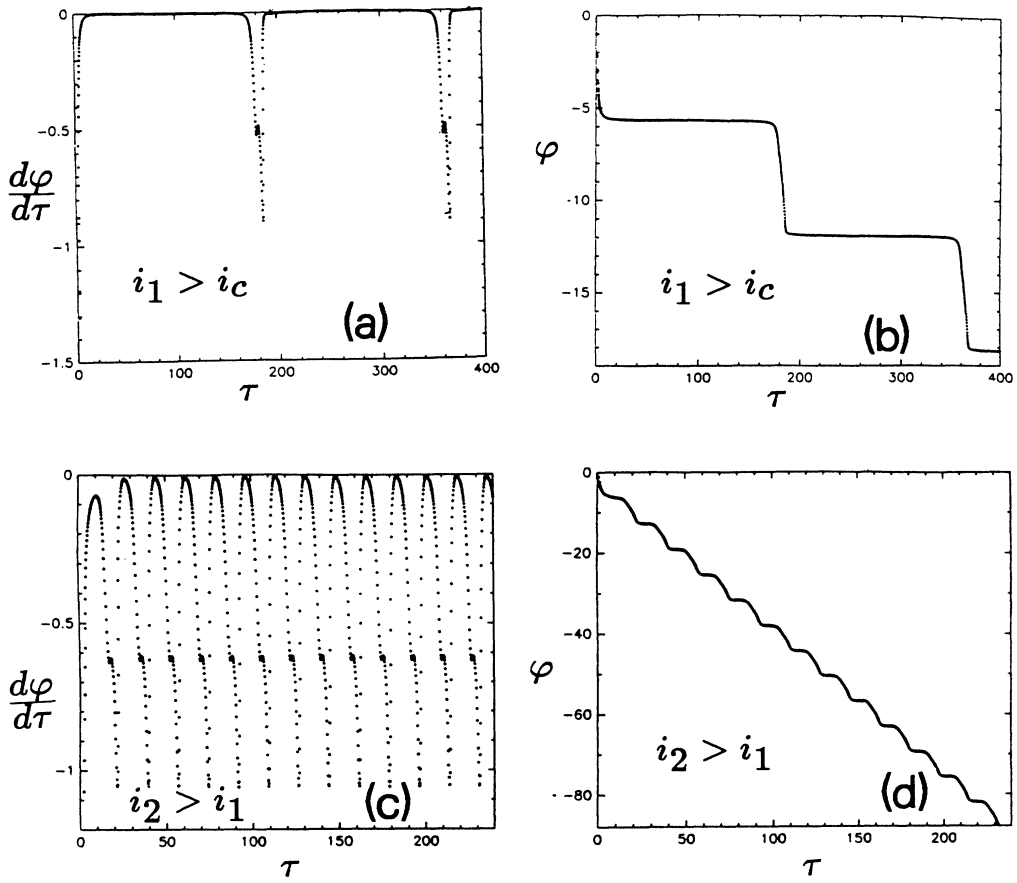

FIG. 4. Phase $\varphi(\tau)$ vs time τ [(b) and (d)] measured at a single site at the top center of a perfect array with a single vertical missing bond ($A=2a$) in the center of the array. The rate of change $d\varphi/d\tau$ vs time τ [(a) and (c)]. Curves (a) and (b) are for a current i_1 just above i_c; curves (c) and (d) are for a current $i_2 > i_1$.

size of the defect. Furthermore, as can be seen in Fig. 4, the individual pulses have a shape that is reflective of the structure of a passing vortex line. As indicated from the numerical simulation, when the current is above and close to the critical current i_c, the *core* of the vortex is just one lattice plaquette, and thus the moving vortices produce a voltage drop only over each junction in the central row. In Fig. 5 we show the region of the sample (i.e., the central row) which carries a normal current and hence a voltage when the current is just above i_c. In Fig. 6 we plot the log of the critical current i_c versus the log of the defect size A for different system sizes. A straight line with slope of $-\frac{1}{2}$ is also drawn. The physical origin of the straight line will be discussed in the next paragraph. One can see that the data points approach the straight line as the defect size A becomes larger and larger. The deviation for very large A is primarily due to the boundaries of the sample since the data points approach the straight line as the sample size is increased. It would be useful to see if this behavior persists to still larger defects and samples, but 51×34 was the largest sample we studied here. This behavior is important for predicting the critical behavior of randomly disordered

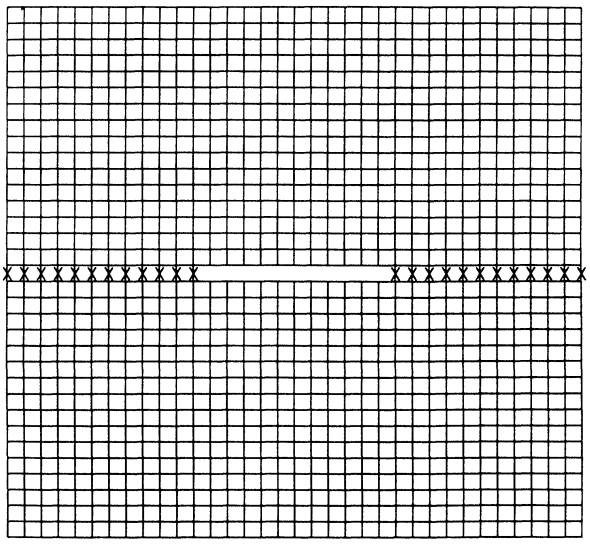

FIG. 5. Perfect 35×34 array with a single linear defect of $A=12a$. The $\times$'s mark those bonds that carry a normal current and that are transversed by the moving vortex lines for current i just above i_c.

arrays.

To obtain the scaling relation between i_c and A (the straight line in Fig. 6), we first estimate the pinning force on the vortex due to the defect and antivortex at the other end. The interaction between vortex and antivortex will be small when compared with the defect pinning energy if the defect is sufficiently long and, normally, can be neglected. Although it is extremely difficult to calculate the pinning force for a vortex outside a rectangular defect, it is reasonable to assume that the pinning force is more or less constant as the length of a long thin defect is changed, while the shape of the end of the defect, near which the vortex is bound, is kept constant. The current enhancement at the tip of the defect, however, is very sensitive to the change of defect length because the external current must all flow around the defect. For a long defect, i_e tends to zero and the Poisson equation can be used to estimate the current enhancement at the defect tip. The current at the tip is given by $i_{\rm tip}=i_\infty[1+(A/2d)^{1/2}]$ for $A\gg d$, where i_∞ is the external current at the boundary.[2] Using the fact that at i_c the Lorentz force equals the pinning force, which is approximately a constant, we have

$$i_c=i_\infty=\text{const}/[1+(A/2d)^{1/2}]\sim A^{-1/2}\ , \tag{5}$$

for $A\gg d$. This scaling relation is the same as that of the random fuse network problem.[2,3]

Rzchowski *et al.*[18] have demonstrated that the discrete nature of a perfect Josephson-junction array is sufficient to pin individual vortex lines in the interstices between sites at low current densities $i_p\sim 0.1 i_0$. Thus, for arrays with sufficiently long defects, corresponding to a vortex depinning current density less than about $0.1 i_0$, the depinning vortex line would move outward away from the defect tip until the enhanced local current density falls below the perfect array pinning current density i_p, at which point the vortex would pin again in an interstitial position of that perfect portion of the lattice. We would not see this phenomenon in our simulations here since, according to Fig. 6, we would have had to study defects of size $A/a\sim 200$ for i_c to fall below $0.1 i_0$. It would be very interesting to study this phenomenon. The important question, relating to whether Eq. (5) is the proper asymptotic form of i_c for discrete Josephson-junction arrays, is what happens next when a vortex line depins from a defect and subsequently is pinned again by the perfect lattice. Would the successive vortices released by the defect pile up behind this first vortex which has been pinned by the perfect lattice? And, assuming so, would this line of vortices extending away from the defect tip act as an extended defect deflecting excess current out to the end of that line of vortices, thereby depinning that last vortex to move still farther out until a path is blazed across the sample? And how will this perfect lattice pinning affect the asymptotic form of Eq. (5)? Of course, this effect will not occur in continuous superconductors, but it would be very interesting to pursue the single defect critical current to very large values of A in discrete arrays, to a few hundred lattice spacings, to test this regime.

When the external current is increased further, we observe that the I-V curve jumps abruptly again at i_{c3} (see Fig. 7). This abrupt jump in the I-V curve is simply due to the creation and motion of additional vortices in the adjacent rows. Thus, as illustrated in Fig. 8, the adjacent rows of junctions immediately below and above the central row develop voltages. These additional vortices are seen, in Fig. 9, near the ends of the defect at different times (in unit of τ) and at $i=0.7065>i_{c3}=0.7045$ on a 35×16 array. The junctions in the central row near the defect carried the most current, and hence the central row was the first to develop voltages (or break down). The next most critical junctions lie immediately above and below in the adjacent rows, and hence the creation of additional vortices here cause these rows to break down next. So, at current i_{c3}, the vortices in the adjacent rows begin to move and produce additional voltages in the

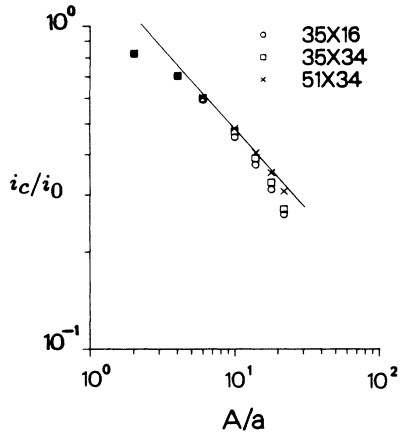

FIG. 6. Critical current i_c/i_0 is plotted vs linear defect size A/a. The data points are from numerical calculations, and the solid line has a slope of $-\frac{1}{2}$. The linear defect in the center of each rectangular sample was aligned parallel to the long axis and perpendicular to the external applied current.

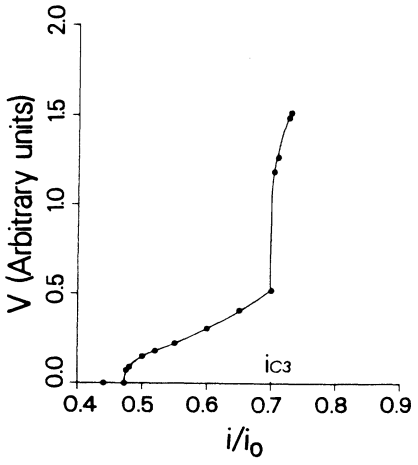

FIG. 7. I-V curve of a perfect array with a single defect of length $A=10a$.

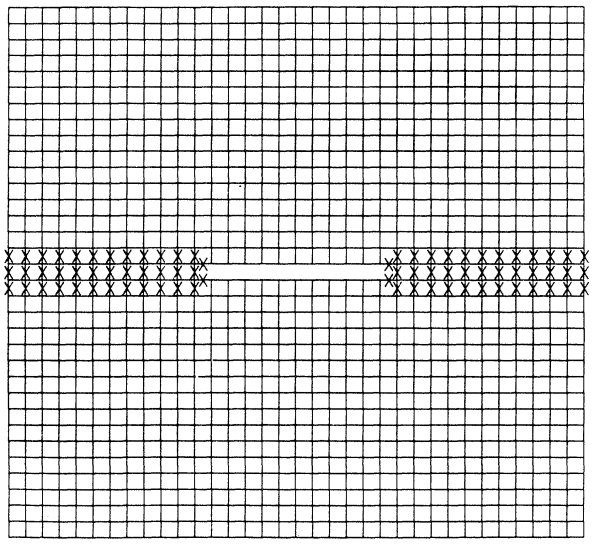

FIG. 8. Perfect 35×34 array with a single defect of length $A=12a$. The ×'s mark those bonds that carry a normal current and that are transversed by moving vortex lines for current i just above i_{c3}.

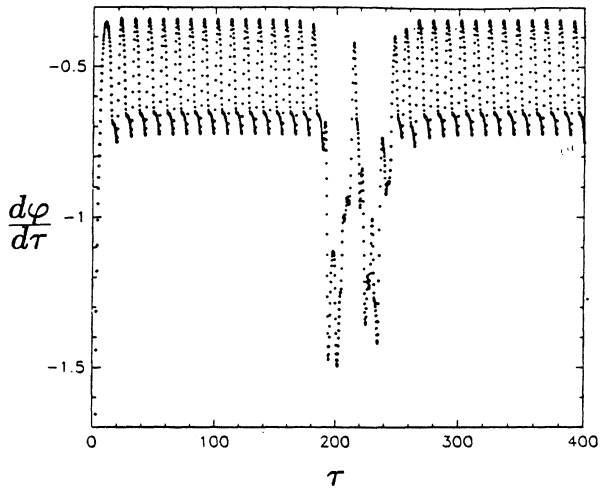

FIG. 10. Rate of change of the phase $d\varphi/d\tau$ vs time τ for a perfect array with a single missing bond ($A=2a$), for current i just above i_{c3}. The chaotic appearing phase corresponds to the time when there are moving vortices, not only in the central row, but also in the adjacent rows.

sample. In the cases where the vortices are formed and depinned at different frequencies in the three rows, we find that $d\varphi/d\tau$, monitored at the top of the system, will have a different and complicated oscillating pattern at each different external current i. At i very close to i_{c3}, $d\varphi/d\tau$ will have a oscillating pattern which switches intermmitently in time; i.e., a plot of $d\varphi/d\tau$ shows a train of periodic oscillations which is disrupted by chaotic appearing intervals as is shown in Fig. 10. Such oscillating patterns occur because the periodic oscillations due to the vortex motion in the central row are superimposed with the oscillations from the vortex motion in the adjacent rows. The fact that the bursts appear to be chaotic instead of periodic is due to the interaction between the vortices in different rows. As the external current i is increased further, the periods of the vortex motion in the adjacent rows become shorter. The oscillating patterns at larger values of current i are periodic if T_1/T_2 is a simple rational number, quasiperiodic if T_1/T_2 is close to a simple rational number, and chaotic otherwise, where T_1 and T_2 are the periods of vortex motion in the central and adjacent rows, respectively. Presumably, there are similar and smaller jumps in the I-V curve as additional rows produce vortices and voltage drops, but we could not resolve these features, although we did observe at higher currents that additional rows develop voltages before the whole system breaks down.

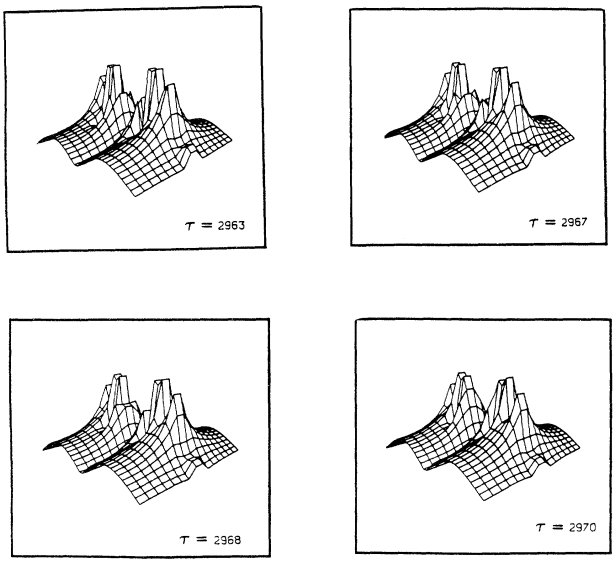

FIG. 9. Snapshots oi vortex movement in a 35×34 array with a single linear defect ($A=10a$) at $i>i_{c3}$ when vortices appear the central row and adjacent rows. The plot is of the supercurrent in the horizontal bonds vs position in the array.

B. Funnel defects

Next, we studied the funnel defect as shown in Fig. 11. This defect has been proposed as a critical defect in the fuse network breakdown problem.[19] This defect is shaped cleverly to funnel large currents through the central neck and therefore to cause the neck to break down at lower external currents. Our initial interest here was to see if we could make the neck region become normal (by the production and annihilation of vortex-antivortex pairs in this region). If this were possible, the signature would be Josephson oscillations or pulses in $d\varphi/d\tau$ vs τ, similar to those shown in Fig. 12, having $\langle d\varphi/d\tau\rangle=0$ or zero average voltage (since there would still be a superconducting path across the sample). In fact, this phenomenon does not happen because of the nonlinearity

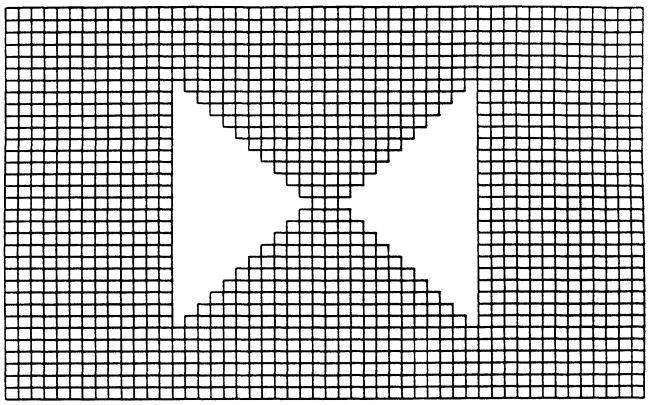

FIG. 11. Perfect 34×51 array with a funnel defect of size $A=10a$.

except when forced by boundary conditions (as shall be discussed later). At lower external current the linear model is correct, the funnel works, and current enhancements produce an incipient vortex-antivortex pair at the inner central points of the funnel as can be seen in Fig. 13(a). But as the external current is increased, the current enhancement on the central points in the neck saturates, near the critical value at which the central vortices would depin, and all additional current is diverted around the entire funnel until the vortices on the external corners become critical [see Fig. 13(b)], and finally both the interior and exterior vortices depin simultaneously in one grand symphony of vortex motion. In the snapshots of Fig. 14 one can see the internal vortices repeatedly depinning, annihilating, and regrowing, while the four

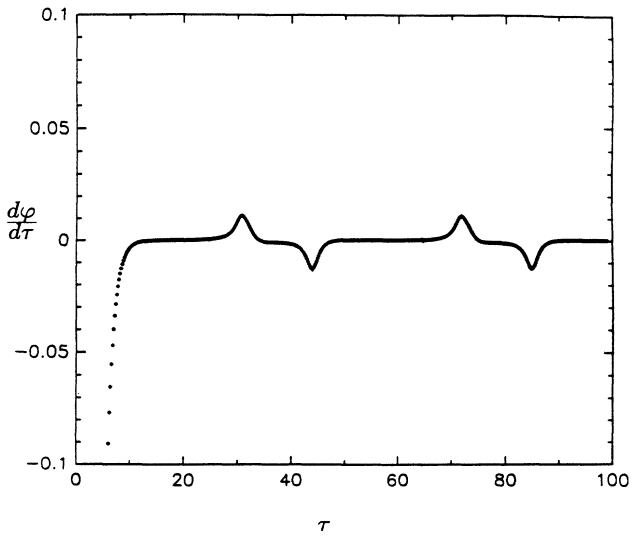

FIG. 12. Example of a plot of $d\varphi/d\tau$ vs τ which shows Josephson oscillations, or pulses, but with (after relaxation on initial conditions) zero average voltage. This curve was produced for the case illustrated later on in Fig. 22.

external vortices are behaving similarly, as a result of the periodic boundary conditions in the horizontal direction. Thus, at the critical current i_c, the voltage (vortex path) appears across the bonds in five locations simultaneously, as is shown in Fig. 15(a). We were able to resolve another transition at a higher current i_{c3} to the state shown in Fig. 15(b), where parades of vortex lines are marching across the bonds indicated, which carry the sample voltage. This behavior, where the breakdown in the neck is held back, by nonlinearity, until there are vortex paths across the entire sample, is obvious in retrospect, but fundamentally very unlike the local breakdown seen in linear problems. We shall call this phenomenon global breakdown. Clearly, if the neck of the funnel were to become normal before the region on the outside of the funnel, then the outside region would be a superconducting short and all the current would go that route, which would cause the neck to become subcritical and superconducting again. There may be circumstances or models where this situation would cause oscillations in the current between the interior and exterior regions, but at least in this RSJ-junction model, as the external current increases, the interior neck region simply approaches criticality, a form of self-organized criticality, and waits with the vortices about to depin, while all the increasing excess current is detoured around the outside until a critical path of vortices across the sample can break loose at once. Finally, we attempted to measure the dependence of the critical current i_c on the size of the funnel defect. The numerical results for i_c vs $2(A/a)$ are shown in Fig. 16, where (A/a) is the number of columns with missing vertical bonds on one side of the funnel. For example, the defect shown in Fig. 15 has $A=4a$, or four columns have missing bonds on one sides of the funnel, and so $2(A/a)=8$ columns counting both sides of the funnel. The straight line has a slope of $-\frac{1}{2}$, showing that Fig. 16 is not incompatible with Eq. (5), although it is also not incompatible with a slope of -1. It was not possible at this time for us to carry out calculations on larger systems than 25×25, and so this result is not definitive, for the value α of the slope.

IV. RANDOMLY DISORDERED ARRAYS

In this section we shall consider an ensemble of randomly diluted arrays of RSJ junctions. In this model each bond in a perfect square lattice is occupied with probability p, above the percolation threshold p_c (i.e., $p_c<p<1.0$), by RSJ junctions. All junctions are identical. The remaining fraction $(1-p)$ bonds are missing. All samples reported in this section were 25×25 at the concentration $p=0.90$ occupied bonds. A typical, computer-generated, randomly diluted array is shown in Fig. 17. Next, we apply a uniform external current i^{ext} into the top nodes of the array and out of the nodes at the bottom, and the dynamical equation (3) is solved numerically. In each case, for current below the critical current $i^{\text{ext}}<i_c$, we find current enhancements (incipient vortex lines) pinned to each random defect in the array. Thus as can be seen in Fig. 18, we see an entire forest of incipient vortex lines, regardless whether we plot the supercurrent

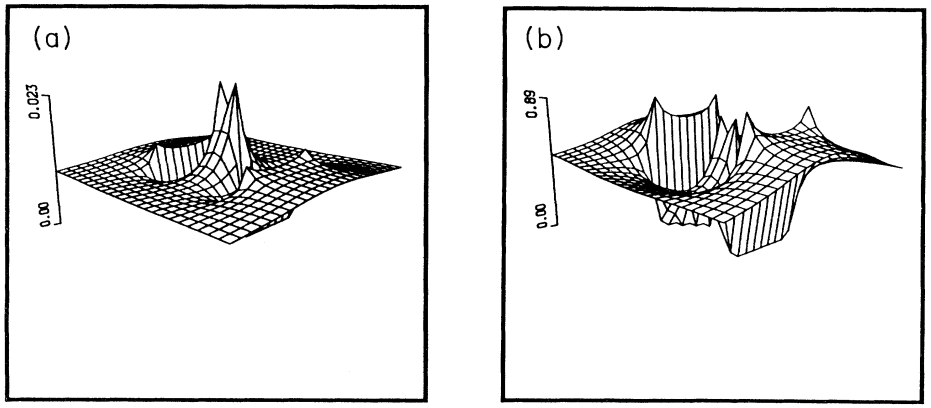

FIG. 13. Snapshots of the supercurrent in the horizontal bonds for small $i < i_c$ in a 25×25 perfect array with a modest-sized ($A = 5a$) funnel defect. Curve (a) is for $i = 0.01$, curve (b) is for $i = 0.5$, and $i_c = 0.565$. These curves are constant in time τ.

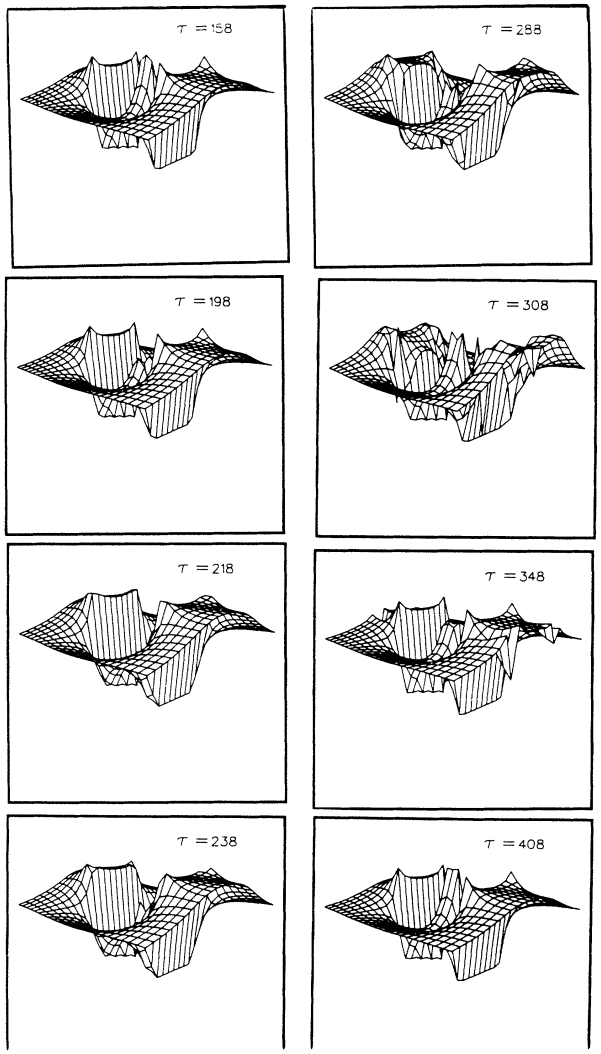

FIG. 14. Snapshots of the supercurrent in the horizontal bonds in a 25×25 perfect array with an $A = 5a$ funnel defect for various times τ, at current $i = 0.60$, just above $i_c = 0.565$.

in each horizontal bond [Fig. 18(b)] (as we did in the single defect cases of Sec. III above) or whether we plot the net current around each nearest-neighbor square or plaquette [Fig. 18(a)]. As the current i is increased and reaches the critical current i_c, vortex and antivortex lines

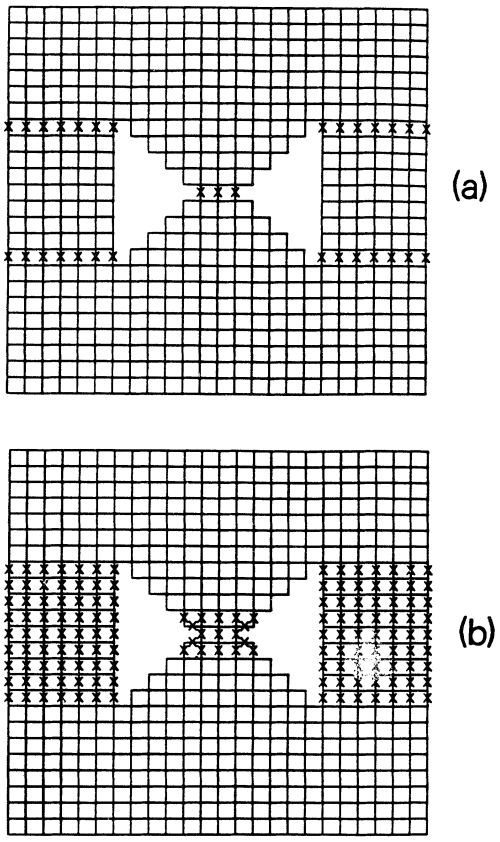

FIG. 15. For the $A = 5a$ funnel defect in a perfect 25×25 array, the $\times$'s mark the paths of the moving vortex lines, or the bonds with normal current, for (a) current i just above i_c and (b) current i just above a higher transition current i_{c3}.

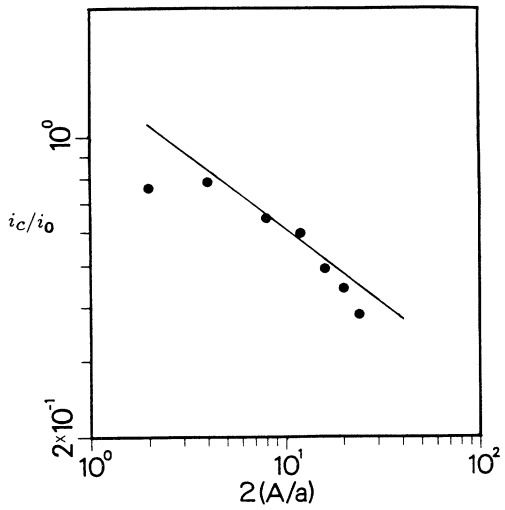

FIG. 16. Critical current i_c/i_0 vs funnel defect size $2(A/a)$ on a logarithmic scale. The data points are from numerical calculations on 25×25 arrays, and the solid line has a slope of $-\frac{1}{2}$.

in a region of the sample depin from their respective defects and travel across the sample, tracing out a breakdown path across which a voltage appears. But to see the few moving vortex lines in the forest of pinned vortex lines is difficult with plots like those of Fig. 18 (unless, perhaps, a movie were made of the motion). Thus we

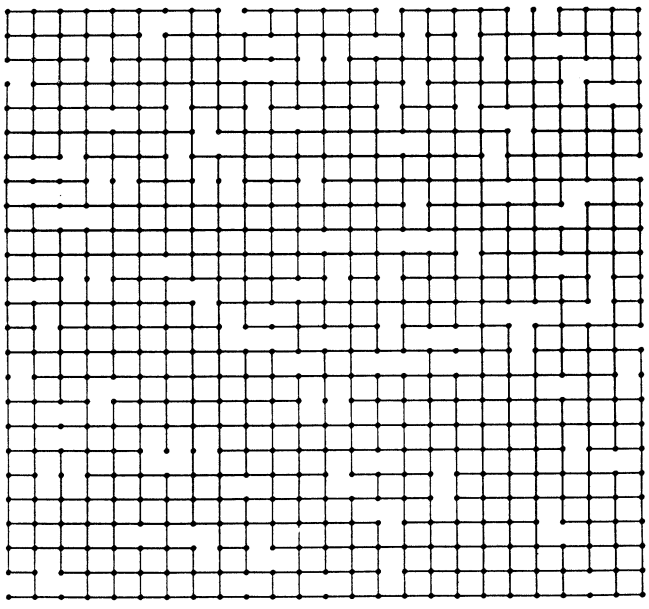

FIG. 17. Typical configuraton of randomly missing bonds (junctions) in a 25×25 array with a probability $p=0.90$ that any bond is present.

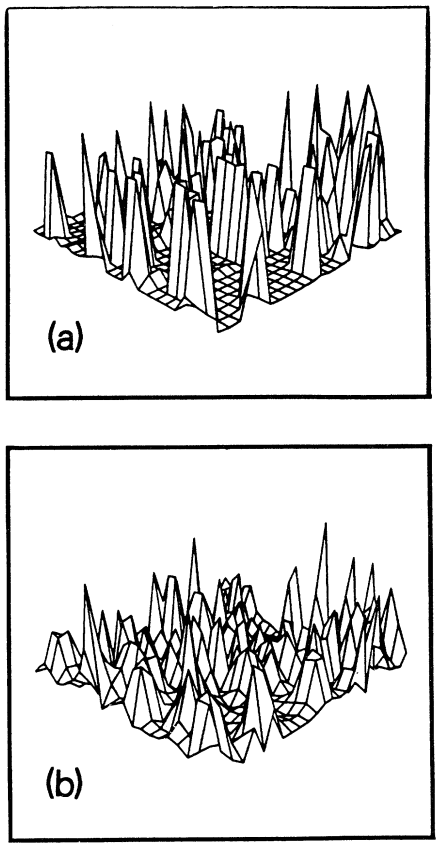

FIG. 18. Snapshots of the current enhancement or incipient vortex lines pinned to defects and moving vortex lines in a 25×25 random array at $p=0.90$ at one time τ. Plot (a) is of the net supercurrent around each nearest-neighbor square or plaquette vs position; plot (b) is of the supercurrent in the horizontal bonds vs position (as was also done previously in Figs. 3, 9, 13, and 14).

have resorted to a plot of the normal current in the horizontal bonds as is shown in Fig. 19 where snapshots of the normal current (in horizontal bonds) are shown at various times. This graphical procedure shows nothing for $i<i_c$ (since there is no normal current or no $\langle d\varphi/d\tau\rangle$) and thus is not useful for studying the precursors to the breakdown, but does clearly show the breakdown path and moving vortex lines for $i>i_c$. A typical breakdown path approximating the vortex motion sequences of Fig. 19 is shown in Fig. 20. In this breakdown path the first vortex motion (normal current) appeared at the solid square in the third column from the left and spread in a complicated manner in both directions across the sample. The path bifurcated near the right-hand edge of the sample, for a current i just above i_c; it is conceivable that this bifurcation occurred very slightly above i_c, although it seemed in our calculation to occur simultaneously with the breakdown just at the initial current. A most obvious feature of the vortex motion in Fig. 19 is its irregularity. Indeed, the vortices seemed to move in fits

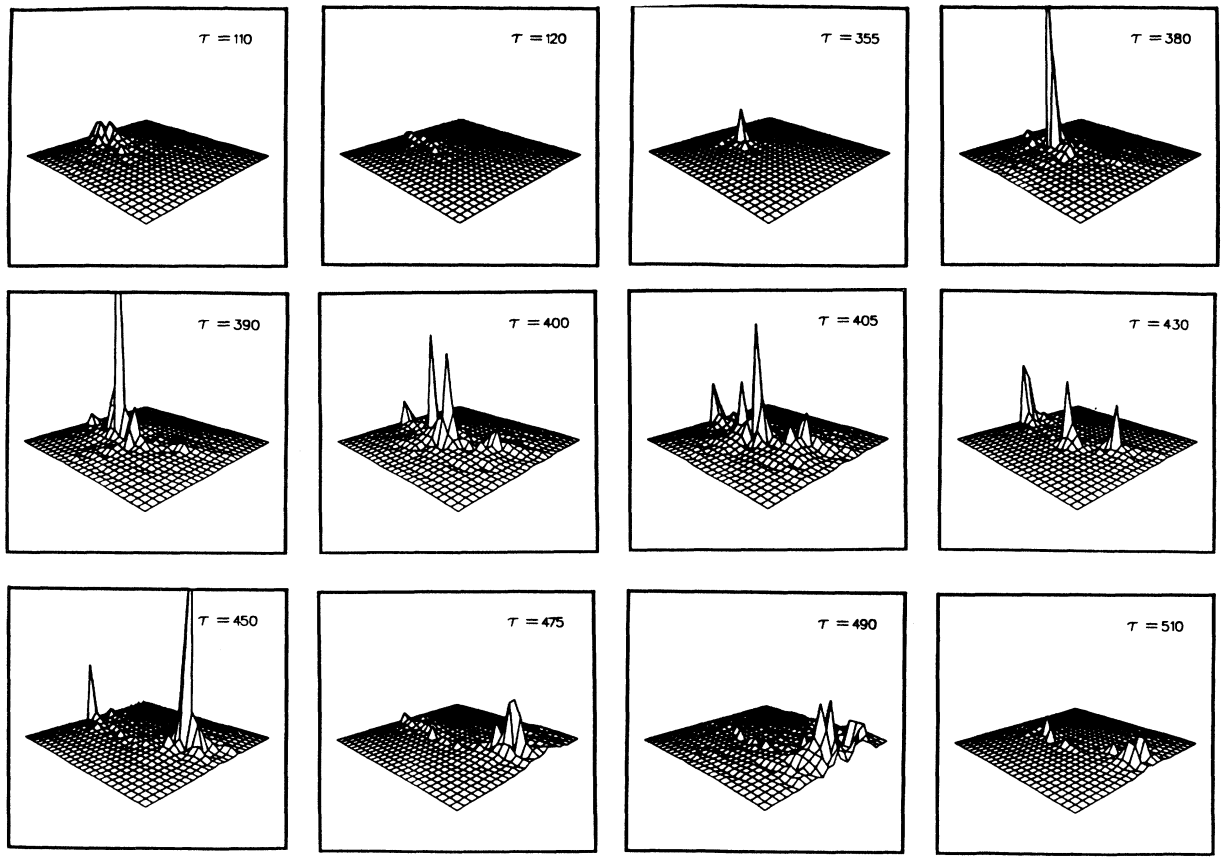

FIG. 19. Snapshots of the normal current in the horizontal bonds vs position in the 25×25 array of Fig. 17 at $p=0.90$, for $i > i_c$, for various times τ.

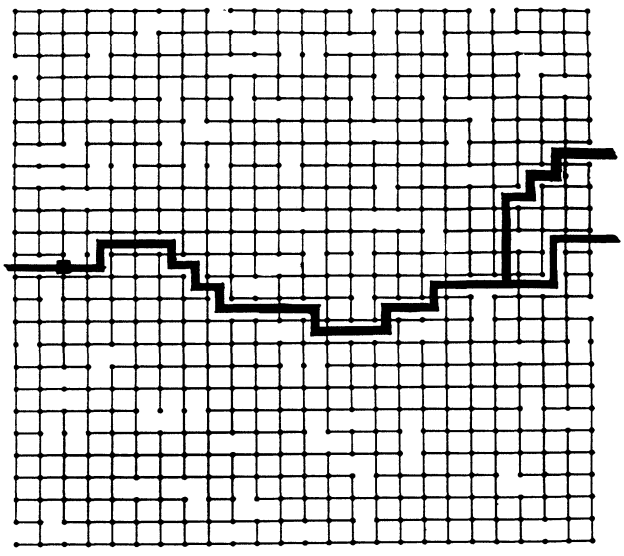

FIG. 20. Approximated path of the vortices or breakdown path for $i > i_c$ in the 25×25 array of Fig. 17. The solid square in the third column marks the point of the first vortex motion which spreads across the sample in an irregular manner.

and starts with great variations or noise in the magnitude of the normal current at any given time. This feature gave rise to very irregular voltage or $(d\varphi/d\tau)$ versus time curves as monitored at a single site. A typical example of $d\varphi/d\tau$ vs τ for a randomly diluted array at $p=0.9$ is shown in Fig. 21. These irregular curves should appear in real experiments as noise, rather than the periodic signals with well-defined frequencies, as are produced by vortices in perfect systems with a single defect, for example. It would be interesting and important to study the frequency dependence of this noise and its variation with the applied current. These calculations and the previous ones above for the funnel defect make clear the importance of global breakdown in randomly disordered superconductors as opposed to the local breakdown that occurs in fuse networks or other linear systems. Because of the nonlinearity, the most critical defect does not simply break down first, but instead waits in a state of criticality for a higher external current i when there can be a breakdown path entirely across the sample. That is, as the external current is increased, one region of the sample after another goes critical or nearly critical (critical here means simply that vortices are ready or nearly ready to depin from their adjacent defects), the excess current (as

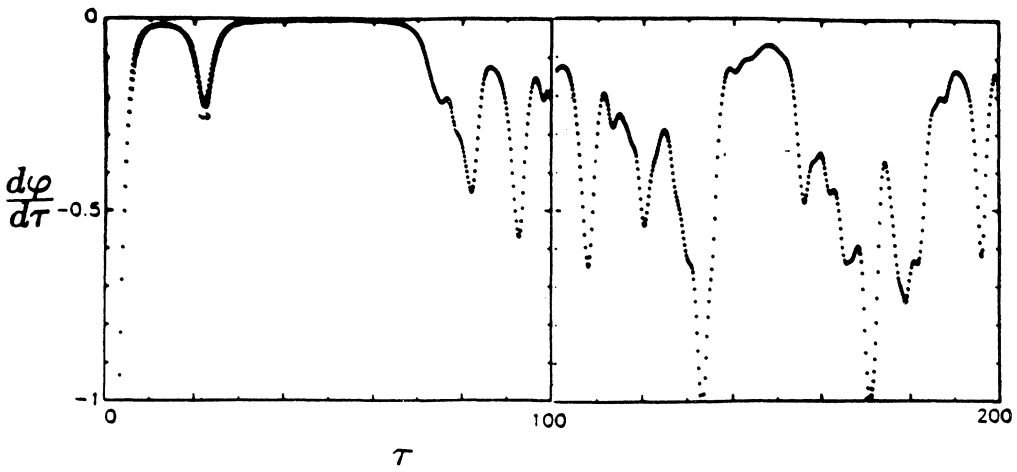

FIG. 21. Typical plot of $d\varphi/d\tau$ vs τ for i just above i_c in a 25×25 random array at $p=0.90$.

the external current is increased further) then avoids these critical regions as long as possible until the critical regions percolate across the sample at which point they can no longer be avoided by the current, and breakdown occurs with a voltage appearing in a path (the percolating cluster) across the entire sample. At first thought one might think that this nonlinear breakdown would fundamentally change the statistics of breakdown. In the linear problem the theory of breakdown is based upon the statistics of extremes. That is, the largest (or most critical) local defect or cluster of defects nucleates the crack or local breakdown, which proceeds to fracture or spread across the network due to the current enhancement (or stress enhancement) at the edge of the crack. Thus the process is dominated by the probability of the occurrence of a local critical defect. In the case of the RSJ array, the critical defect is held back by nonlinearity from becoming normal until a complete or global vortex trail or path across the sample can be blazed through the percolating critical regions. But, perhaps, this picture underplays the still-pivotal role played locally by the most critical defect or cluster of defects.

Consider for a moment the low concentration $[(1-p)\rightarrow0]$ limit. Here, clearly, one can still consider single defects (of missing junctions) just as in the linear problems. Indeed, the critical current behavior with a single large defect (see Fig. 6) still is seen to decay as a power of the defect size. And clearly the Liftshitz arguments used previously in the linear cases still apply. That is, the probability of occurrence of a large cluster of defects decays exponentially with cluster size. Thus, at least at low concentration of defects, one still obtains the previous logarithmic vanishing[2] of the breakdown current i_c in the thermodynamic limit, i.e.,

$$i_c \propto 1/[1+K(\ln L)^{\alpha}] , \tag{6}$$

where K is a defect concentration-dependent constant and the power α is a constant of order 1. Similarly, as shall be described below, the statistics of extremes gives a characteristic modified Gumbel form to the critical current distribution in an ensemble of random samples. But as the concentration of missing junctions $(1-p)$ increases, we need to consider the effect of the nonlinear interactions between defects or clusters of defects. Despite the fact that the vortex path must percolate entirely across the sample, this percolation seems to happen rapidly, once the largest defect has gone critical, and thereby blocks a large region of the sample from carrying any additional current. The excess current is diverted away to the regions to each side of the critical defect, and this feature seems to quite rapidly cause them to saturate or become critical so that the dominant determinant of the breakdown still seems to be the most critical defect or cluster of defects which nucleate the global spreading of the criticality. Thus the statistics of extremes should still apply. This, which we have tested numerically, is discussed below. Indeed, for linear breakdown problems in most of the numerical simulations in the literature (note especially Fig. 8 and the related discussion in Duxbury, Leath, and Beale[2]), the current i, at which the the first bond breaks, and the current i_b, at which the entire network breaks, seem to scale in the same manner. And, moreover, for very large samples, the network breaks very close to the breaking of the first few bonds. In the RSJ-junction array case here, what seems to be happening is that i_1 is simply pushed up to i_c (analgous to i_b). That is, although the first defect to reach the critical status locally cannot go normal until i_c is reached, nevertheless, for large samples, global breakdown seems to follow very closely to the criticality of the first most critical defect region. The picture that emerges here may have substantial experimental consequence in experiments on real granular (or other disordered) superconducting thin films with a dc bias voltage applied. In particular, near the critical current i_c, there may be large regions of the sample in a critical state, where the vortex lines in these regions are just about to depin from their associated defects.

Thus, for example, if superconducting samples in the state of criticality were stimulated by some external source, such as laser light or microwave radiation, one would expect an anomalously large depinning of vortex lines and, hence, voltage and noise and other responses in the system. In particular, the motion of these vortices in disordered systems is extremely noisy, and this may be an explanation for the anomalously large amount of noise seen experimentally in some dc-biased Josephson-junction systems[20] and for the anomalous photoresponse seen in granular superconducting thin films.[21]

Before giving our statistical data, there is one important aside to be discussed. In Fig. 12 we show a curve of $d\varphi/d\tau$ vs τ which shows Josephson oscillations but zero average voltage (after the transient from the initial conditions disappears). This curve and a number of similar ones were actually seen in the data for randomly diluted arrays for a few configurations of defects that occurred randomly within the ensemble. In each such case of oscillations with zero average voltage, a map of the locations of these oscillations (locally produced and annihilated vortex-antivortex pairs) showed that the oscillations were occurring at the top or bottom edges of the sample (there are periodic boundary conditions on the sides). A typical snapshot of the behavior is shown in Fig. 22. This behavior was being forced by our boundary conditions, which require equal current into (or out of) each node at the top (or bottom) of the sample. And in a few cases this boundary-imposed current could only be carried, as a result of the local configuration of missing bonds, by passing through a local funnel-shaped region, which then had to become normal. Therefore, so as not to systematically bias the data, we attached bus bars (three perfect rows of junctions) to the top and bottom of each otherwise randomly diluted array in the ensemble. This change of boundary conditions eliminated all oscillations with zero average voltage.

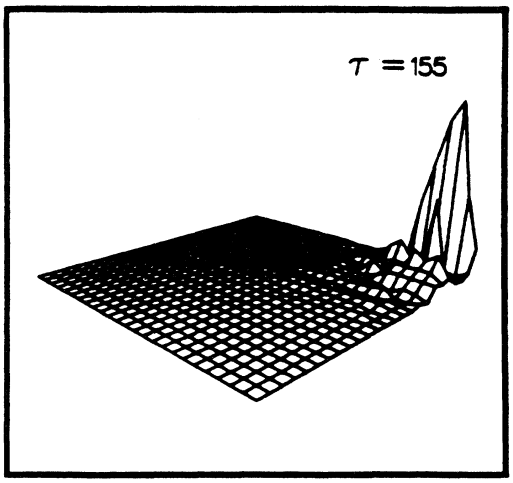

FIG. 22. Snapshot of the normal current in horizontal bonds corresponding to the case in Fig. 11 where there are Josephson oscillations but no average voltage. The vortex creation, motion, and annihilation are confined to the region shown at the top of the sample. Such cases were eliminated by adding bus bars to the samples.

We then proceeded to measure the critical current i_c for an ensemble of 800 randomly diluted arrays which were 25×25 (plus the perfect 3×25 bus bars at top and bottom) at $p=0.90$. The resulting failure distributions $F(i)$ (the probability that a sample has a critical current $i_c<i$) gives the usual S-shaped curve shown in Fig. 23. It would have been nice to have demonstrated directly the logarithmic vanishing [Eq. (6)] of $\langle i_c \rangle$ in the thermodynamic limit of $L\to\infty$, but the available computer time limited the sample size so that the required several orders of magnitude in sample size L (or even a few) could not be investigated. The alternative is to consider the shape of the failure distribution $F(i)$ and compare it with the various predictions from the statistics of extremes. There are basically two fixed points in the form of $F(i)$, which are discussed by Duxbury, Beale, and Leath[2] and originally by Gumbel.[4] The first is what we shall call the modified Gumbel (MG) distribution

$$F_{\mathrm{MG}}(i)=1-\exp\{-CL^d\exp[-(k/i)^{1/\alpha}]\}\ , \tag{7}$$

where C and k are constants that are determined by details of the vortex depinning process, where d is the dimension of the system ($d=2$ in this case) and where α is the exponent that would apply (as in Fig. 6) for the critical defect of defect clusters. This general form was found to fit a wide variety of applications to breakdown of linear systems.[1–3,5] It arises whenever the extreme event, the existence of the critical defect or cluster of defects, has an exponentially small probability with increasing defect or cluster size. The second fixed point function is given by the Weibull (W) distribution[4]

$$F_W(i)=1-\exp(-cL^d i^m)\ , \tag{8}$$

where c and the exponent m are constants, and where d is the dimension of the system ($d=2$ here). This Weibull form (8) has been used widely in engineering applications for years[22] and, especially for large m, is difficult to distinguish from the modified Gumbel form (7) except in the toe (small-i) region. In order to fairly distinguish between the two curves from our data in Fig. 23, we calculate the quantity

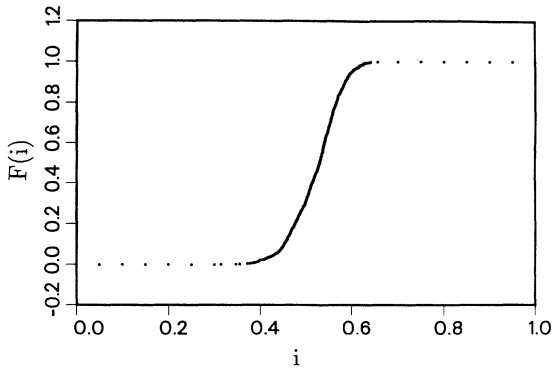

FIG. 23. Failure distribution $F(i)$ vs i for the ensemble of 800 random 25×25 arrays at $p=0.90$.

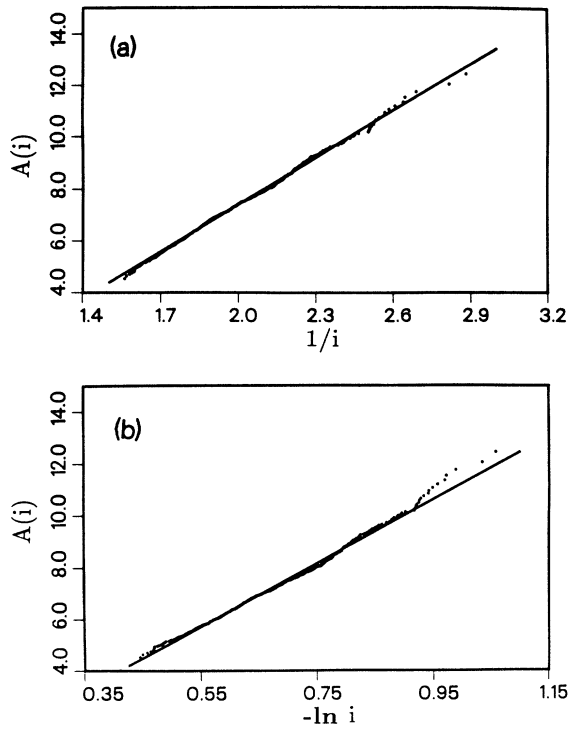

FIG. 24. Plot of $A(i)$, as given by Eq. (9), vs $1/i$ [curve (a)] which is a test of the modified Gumbel distribution [Eq. (10)], and $A(i)$ vs $\ln i$ [curve (b)] which is a test of the Weibull distribution [Eq. (11)].

$$A(i)=-\ln\{-\ln[1-F(i)]/L^d\} \ . \tag{9}$$

From Eqs. (7) and (8), we thus obtain

$$A_{\rm MG}(i)=(k/i)^{1/\alpha}-\ln C \tag{10}$$

and

$$A_W(i)=-m\ln i-\ln c \ . \tag{11}$$

Actually, since α is of order of 1 and since we have data only over a relative small range of i, we cannot definitively determine α. For simplicity and because it seems to fit the data best, we shall assume $\alpha=1$ for our purposes here. The resulting plots of $A(i)$ vs i are shown in Fig. 24. In Fig. 24(a) we show $A(i)$ vs i^{-1} as a test of the modified Gumbel distribution (10), whereas in Fig. 24(b) we show $A(i)$ vs $\ln i$ as a test of the Weibull distribution (11). Any deviation would be expected only on the low-i (high-i^{-1}) end. The results suggest that the modified Gumbel distribution fits best, although these results are not as clear as those obtained previously for 50×50 fuse networks.[2] It will take calculations on samples larger than 25×25 to give definitive results here.

It is obvious, but perhaps worth noting, that the nature of the vortex breakdown path that occurs varies considerably as one goes from the toe (the bottom) of the S-shaped curve of $F(i)$ in Fig. 23 to the shoulder (the top) of the curve. Those random samples which have low critical current i_c [a typical sample with $i_c=0.38$ is shown in Fig. 25(a)] tend to have strategically placed vacancies across the sample so that only a few junctions need become normal at i_c, and the vortex path tends to be a rather straight line across the sample. For samples in the middle of the curve [a typical sample with $i_c=0.56$ is shown in Fig. 25(b)] more junctions become normal at i_c and the vortex paths are more tortuous. Finally, for samples in the shoulder of the curve [a typical sample with $i_c=0.64$ is shown in Fig. 25(c)], there are many junctions which must become normal for the transition to occur and the path is quite tortuous and, perhaps, even fractal. Although this fact seems obvious, it does not seem to have been noted before (despite the fact that similar process must occur in the failure distribution of virtually all breakdown problems).

Finally, we have studied the average I-V characteristics for an ensemble of 400 randomly diluted arrays of 25×25 junctions at $p=0.90$. In Fig. 26(a) we plot the average voltage $\langle V\rangle$ for the ensemble versus applied current i (solid circles) and the root-mean-square voltage

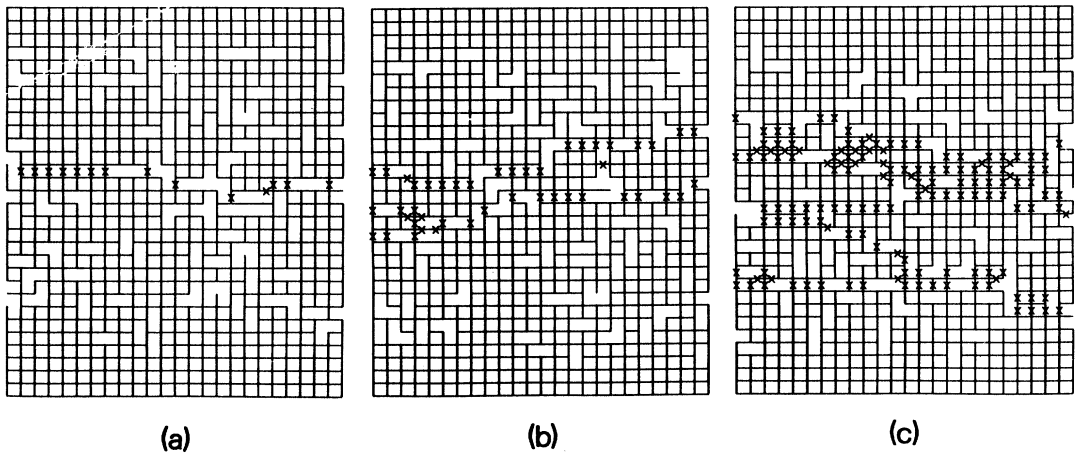

FIG. 25. Typical vortex breakdown paths for i just above i_c on random 25×25 arrays, at $p=0.90$. Sample (a) had $i_c=0.38$, sample (b) had $i_c=0.56$, and sample (c) had $i_c=0.64$.

$V_{\rm rms}$ vs i (open circles). As has previously been discussed,[5] many experimental voltage-current measurements[23] and calculations[24] in granular superconductors have been modeled over the years. These authors have reported a voltage-current relation just above a critical value $i_{\langle v\rangle}$, which behaves according to the empirical formula

$$V/L \propto (i-i_{\langle v\rangle})^x , \tag{12}$$

where $i_{\langle v\rangle}$ is the critical current for the ensemble and where, in two dimensions, x approaches 3.0 as $T\rightarrow T_c$. Our calculations here correspond to $T=0$ in the RSJ-junction array. Nevertheless, we considered the data for $\langle V\rangle$ in Fig. 26(a) and treated $i_{\langle v\rangle}$ as a parameter, varying it to get the best straight line for $\ln V$ vs $\ln(i-i_{\langle v\rangle})$. The result shown in Fig. 26(b) nicely fits a straight line corresponding to $x=3.1\pm0.1$. The slope of the straight line in Fig. 26(b) is 3.1. This result is consistent with that from the linearized model.[5]

Finally, there is the question of whether, in the thermodynamic limit, in two-dimensional arrays with dilute randomness, there is still a finite-temperature Kosterlitz-Thouless phase transition. The result seems to show that there clearly is, since the exponent x above is clearly bigger than one. That is, in the thermodynamic limit where $i_c\rightarrow 0$, the linear resistivity is also zero; hence the material may still be considered to be superconducting. That is, when a voltage first appears, it is only in a very small number of regions of the sample, and hence the voltage density or average electric field across the sample is negligible.

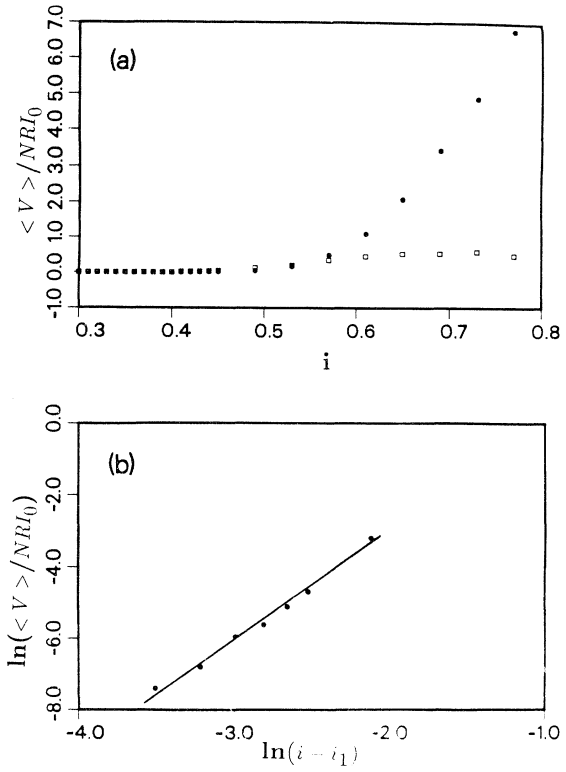

FIG. 26. (a) I-V curve for the average voltage $\langle V\rangle$ (solid circles) and for the standard deviation of the voltage. $V_{\rm rms}$ (open circles) for an ensemble of 400 arrays (25×25) at $p=0.90$. (b) Logarithmic plot of $\langle V\rangle$ vs $\ln(i-i_{\langle v\rangle})$, where $i_{\langle v\rangle}$ is treated as a parameter to get the best straight-line fit to the data. The straight line has a slope of $x=3.1$ for $i_{\langle v\rangle}=0.40$.

V. CONCLUSION

We have numerically studied the onset of voltage at the critical current in disordered arrays of resistively shunted Josephson junctions at zero magnetic field and zero temperature. The breakdown of the coherent superconducting state at i_c is different in several fundamental ways from that of the linear systems previously studied, systems such as fuse network breakdown, brittle fracture, dielectric breakdown, and onset of critical current in linearized superconducting models. First, the breakdown here is seen to be caused by vortex line depinning from the defects in the sample. This process occurs spontaneously and naturally in the solutions of the dynamic RSJ-junction equations. In addition, for the case of single large defects, we observed a series of transitions as the sample broke down row by row with parades of vortex lines crossing those rows with voltage. Second, a confined region of the sample does not go normal until a spanning region or vortex breakdown path can occur across the entire sample. Finally, despite the nonlinearities, the statistics of the failure rate of the RSJ-junction arrays appears to be remarkably similar to that of the linear models. In particular, we predict that the critical current in disordered superconducting systems will go to zero logarithmically in the thermodynamic limit.

ACKNOWLEDGMENTS

We are grateful to Michael J. Stephen for stimulating discussions and helpful suggestions. We also would like to thank Philip M. Duxbury, William L. Mclean, T. Venkatesan, and David Stroud for useful conversations. The support of the National Science Foundation through the Pittsburgh Supercomputing Center and John von Neumann Supercomputer Center is also gratefully acknowledged.

[1]L. de Arcangelis, S. Redner, and H. J. Hermann, J. Phys. Lett. (Paris) **46**, L585 (1985).

[2]P. M. Duxbury, P. D. Beale, and P. L. Leath, Phys. Rev. Lett. **57**, 1052 (1986); P. M. Duxbury, P. L. Leath, and P. D. Beale, Phys. Rev. B **36**, 367 (1987).

[3]M. Sahimi and J. D. Goddard, Phys. Rev. B **33**, 7848 (1986); P. D. Beale and D. J. Srolovitz, *ibid.* **37**, 5500 (1988).

[4]E. J. Gumbel, *Statistics of Extremes* (Columbia University

Press, New York, 1958).
[5]P. L. Leath and W. Tang, Phys. Rev. B **39**, 6485 (1989).
[6]J. E. Mooij and G. Schön, Physica B **152**, 1 (1988).
[7]C. J. Lobb, D. W. Abraham, and M. Tinkham, Phys. Rev. B **27**, 150 (1983).
[8]K. A. Muller, M. Takashige, and J. G. Bednorz, Phys. Rev. Lett. **58**, 1143 (1987); M. Tinkham, *ibid.* **61**, 1658 (1988); Y. Yeshurun and A. P. Malozemoff, *ibid.* **60**, 2202 (1988).
[9]W. Xia and P. L. Leath, Phys. Rev. Lett. **63**, 1428 (1989).
[10]W. Xia and P. L. Leath, Bull. Am. Phys. Soc. **36**, 724 (1991).
[11]S. R. Shenoy, J. Phys. C **18**, 5163 (1985); K. K. Mon and S. Teitel, Phys. Rev. Lett. **62**, 673 (1988); J. S. Chung, K. H. Lee, and D. Stroud, Phys. Rev. B **40**, 6570 (1989).
[12]Ch. Leemann, Ph. Lerch, B. A. Racine, and P. Martinoli, Phys. Rev. Lett. **56**, 1291 (1986); R. K. Brown and J. C. Garland, Phys. Rev. B **33**, 7827 (1986); B. J. van Wees, H. S. J. van der Zant, and J. E. Mooij, *ibid.* **35**, 7291 (1987); M. G. Forrester, H. J. Lee, M. Tinkham, and C. J. Lobb, *ibid.* **37**, 5966 (1988); also see articles in Physical (Utrecht) **152B**, 1–302 (1988); D. J. Resnick, J. C. Garland, J. T. Boyd, S. Shoemaker, and R. S. Newrock, Phys. Rev. Lett. **47**, 1542 (1981); M. Tinkham, D. W. Abraham, and C. J. Lobb, Phys. Rev. B **26**, 6578 (1983); R. A. Webb, R. F. Voss, G. Grinstein, and P. M. Hom, Phys. Rev. Lett. **51**, 690 (1983); D. Kimhi, F. Leyvrayz, and D. Ariosa, Phys. Rev. B **29**, 1487 (1984).
[13]K. K. Likharev, Rev. Mod. Phys. **51**, 101 (1979).
[14]B. D. Josephson, Phys. Lett. **1**, 251 (1962); Adv. Phys. **14**, 419 (1965).
[15]In some cases, such as random initial conditions, a nonuniform mixture of superconducting and normal current distributions in the vertical direction seems to persist.
[16]D. E. McCumber, J. Appl. Phys. **39**, 3113 (1968); W. C. Stewart, Appl. Phys. Lett. **12**, 277 (1968).
[17]Y. B. Kim and M. J. Stephen, in *Superconductivity,* edited by R. D. Parks (Dekker, New York, 1969), Vol. 2.
[18]M. S. Rzchowski, S. P. Benz, M. Tinkham, and C. J. Lobb, Phys. Rev. B **42**, 2041 (1990).
[19]J. Machta and R. A. Guyer, Phys. Rev. B **36**, 2142 (1987); J. Helsing, J. Axell, and G. Grimvall, *ibid.* **39**, 9231 (1989).
[20]Y. Taur and P. L. Richards, J. Appl. Phys. **48**, 1321 (1977); B. A. Huberman, J. P. Crutchfield, and N. H. Packard, Appl. Phys. Lett. **37**, 750 (1980).
[21]J. C. Culbertson, U. Strom, S. A. Wolf, P. Skeath, E. J. West, and W. K. Burns, Phys. Rev. B **39**, 12 359 (1989); J. C. Culbertson, U. Strom, S. A. Wolf, and W. W. Fuller, *ibid.* (to be published).
[22]W. Weibull, J. Appl. Mech. **18**, 293 (1951).
[23]S. A. Wolf, D. V. Gubser, and Y. Imry, Phys. Rev. Lett. **42**, 324 (1979); A. M. Kadin, K. Epstein, and A. M. Goldman, Phys. Rev. B **27**, 6691 (1983); A. F. Hebard and A. T. Fiory, Phys. Rev. Lett. **50**, 1603 (1983).
[24]C. Lebeau, J. Rosenblatt, A. Raboutou, and P. Peyral, Europhys. Lett. **1**, 313 (1986).